Coaxial SIW Filters – *When compactness meets flexibility*

J.D. Martínez[1], S. Sirci[2], V.E. Boria[3] and M.A. Sánchez-Soriano[4]

[1]I3M, Universitat Politècnica de València, Camino de Vera s/n, Valencia (SPAIN)

[2]SwissTo12, CH-1020 Renens (SWITZERLAND)

[3]iTEAM, Universitat Politècnica de València, Camino de Vera s/n, Valencia (SPAIN)

[4]Department of Physics, Systems Engineering and Signals Theory, University of Alicante, Alicante (SPAIN)

Corresponding author email: jdmartinez@eln.upv.es

Substrate integrated waveguide (SIW) technology [1], [2] is a well-established and successful approach for implementing planar microwave filters with very stringent requirements in terms of Q-factor and ability to integrate into a system. Optimized SIW filters can reach a Q-factor of 200 to 800 using low-loss substrates and standard fabrication procedures [3]. Furthermore, packaging and EM shielding, power handling capabilities, and low-cost batch manufacturing are other broadly recognized strengths of this approach. However, SIW filters are still larger than most of their planar counterparts, while advanced topologies are not always easy to accommodate, and filter reconfigurability usually leads to very complex implementation [4], [5], [6].

Several SIW structures have been developed to overcome these drawbacks. For instance, more compact implementations can be obtained using folded SIW cavities [7] or by loading SIW filters with dielectric rods [8], both at the expense of less standard manufacturing processes. Other techniques have exploited EM field symmetry to create a virtual magnetic wall without requiring a multi-layer manufacturing technology, as in half-mode [9], quarter-mode [10], and even eight-mode [11] SIW structures. Loading of the SIW cavity with complementary split-ring resonators (CSRRs) [12] has also been a

successful approach for further miniaturization. However, some of these approaches can lead to Q-factor degradation due to radiation issues at opened boundaries. For instance, quarter-mode SIW structures can lead to 40% to 60% degradation of the unloaded Q-factor compared to a classic SIW cavity resonator [13].

Finally, a key feature of SIW technology has always been the ability to adapt classical and well-known metallic waveguide structures and topologies to a dielectric-filled planar implementation. Consequently, ridge evanescent-mode filters [14] in SIW technology were originally proposed as a way to achieve further miniaturization without degrading the intrinsic Q-factor while enabling both narrow and wide-band responses. Thus, in [15] an ultra-wideband filter was designed using ridge waveguide resonators defined by periodic via fences, while in [16] the concept was also extended to folded SIWs for extra compactness. Other approaches were based on the introduction of capacitive loading posts inside an SIW cavity resonator [17], [18], [19] or stubs within a below cut-off SIW section [20]. However, additional manufacturing steps for creating a buried capacitive post or multi-layer technologies were required in all of these structures, reducing the cost-effectiveness of this approach compared to standard printed circuit board (PCB) technology.

The introduction of vertical capacitive posts into single-layer SIW cavity resonators was initially proposed in [21] as a way of perturbing the electric field distribution, and thus the resonant frequency of square SIW cavity resonators. As a preliminary concept, several posts were inserted and subsequently connected and disconnected from the bottom ground plane for generating different resonant frequencies, showing very interesting discrete tuning capabilities. This approach was later explored by other

groups for implementing reconfigurable SIW filters using PIN diodes [22] and RF MEMS [3] as switching elements. However, their focus was primarily on determining the best location for the different switchable obstacles inside the cavity, in order to obtain the desired set of resonant frequencies, rather than on the resonator structure itself.

Following this idea, the well-known coaxial (or combline) cavity resonator [23] can be translated from metallic waveguide technology to a single-layer substrate integrated approach. Thus, a properly designed capacitive post, consisting of a short-circuited via hole capacitively loaded at the top by an isolated metal patch, was first proposed in [24], while an equivalent circuit, filter design procedure, and measured results were discussed in [25], hence enabling the realization of single-layer coaxial filters in SIW technology.

The main potential advantages of coaxial SIW structures are:

- By increasing the length of the post or the loading capacitance, a huge size reduction can be achieved compared to conventional SIW cavity resonators.
- Both inductive and capacitive couplings can be achieved on the top layer for obtaining filter responses allocating finite transmission zeros [26]. Moreover, other advanced topologies, such as multi-mode resonators, singlets and doublets, can also be implemented by translating their well-known metallic waveguide counterparts.
- The easy access to the loading capacitance enables the direct integration of lumped capacitors as well as tuning elements, such as varactors, PIN diodes, or RF MEMS.

In the following sections, the basic coaxial SIW filter topology is presented, as well as the latest advances regarding device miniaturization, design flexibility, advanced filtering responses, and implementation of tunable filters based on coaxial SIW structures.

Coaxial SIW Resonator

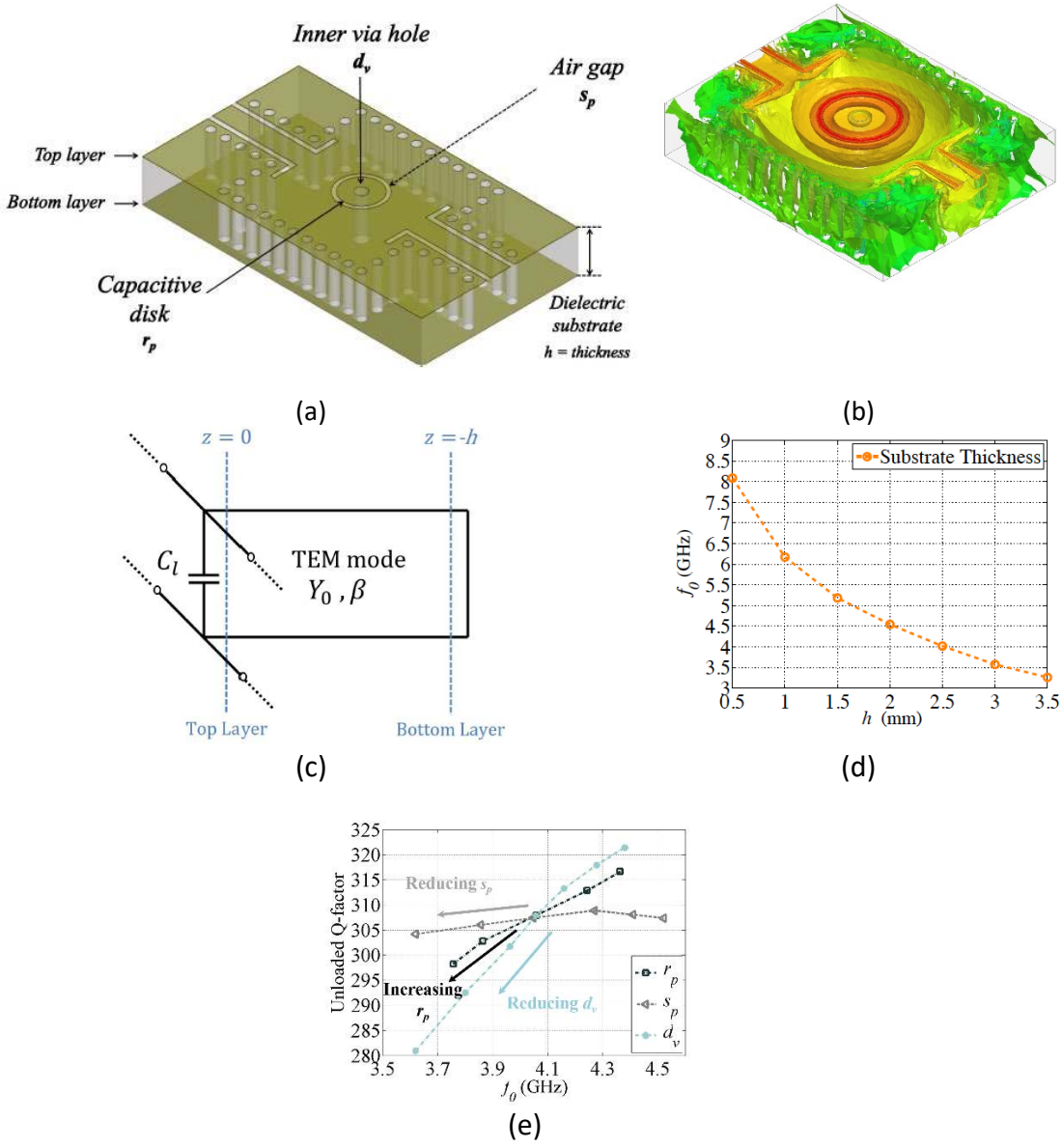

Figure 1. (a) A coaxial SIW resonator, (b) electric field distribution at the top plane, (c) equivalent circuit of the coaxial SIW resonator, (d) resonant frequency as a function of the substrate thickness for a resonator example with the following parameters: 2.554 mm-thick Rogers TMMi (ε_r = 9.8, tan δ = 0.002) with 17 μm base Cu, resonator length 38.2º with C_l = 1.25 pF and resonator impedance Z_0 = 40.8 Ω (i.e. SIW cavity size 6.3 x 6.3 mm^2 with r_p = 2 mm and s_p = 0.125 mm), and (e) variation of the unloaded Q-factor with the main geometrical parameters.

As mentioned above, the coaxial SIW concept was first presented in [24], where the authors proposed the implementation of a combline resonator by introducing a plated via hole at the center of a square SIW cavity. This plated via hole behaves as the inner conductor of a short section of TEM-mode coaxial line along the vertical direction (i.e., the substrate thickness), while the outer conductor is defined by the SIW post wall. In order to define the coaxial resonator, the inner via hole must be short-circuited at the bottom ground plane and finished in a metal patch at the top. A schematic of the structure is shown in Fig. 1(a). The metal patch is then isolated from the top ground plane by an isolating gap, hence introducing an important capacitive load through the established fringing fields, as can be seen in Fig. 1(b).

In [25], a simple model of the structure based on a short-circuited stub in parallel with a lumped loading capacitor was proposed and compared with full-wave EM simulations. The equivalent circuit is shown in Fig. 1(c). The main parameters of the coaxial resonator are the characteristic admittance of the inductive section Y_0, given by the ratio between the inner via diameter d_v and the SIW cavity width W, and the value of the loading capacitance C_l. Given these two parameters, the resonant frequency ω_0 can be obtained by making the resonator susceptance B equal to zero

$$B(\omega_0) = \omega_0 C_l - Y_0 \cot \beta h \tag{1}$$

The agreement of this model with the EM simulations, although a first-order approximation, is still very good and valuable for initial design. The resonant frequency of the structure is very dependent on the substrate thickness h (i.e., the resonator length), as can be seen in Fig. 1(d), thus enabling an enormous size reduction for a given resonator layout.

The values of Y_0 and C_l are both functions of the geometry of the structure. For instance, both square [25] and circular [27], [28] outer SIW cavities have been employed. In both cases, approximate expressions for the characteristic impedance of equivalent coaxial transmission lines are available [29], [30]. Regarding the loading capacitance, different shapes have been used for the top metal patch, including circular [25], rectangular [31], and interdigital [32]. The latter is very interesting when highly loaded resonators are required, even if in this case surface-mount devices (SMDs) could be also employed [33].

The diameter and spacing of the via holes forming the SIW post wall are chosen through the same design criteria followed in classical SIW technology [34]. The dimensioning of the structure for a given resonant frequency (once the substrate material and dielectric thickness have been chosen) starts by choosing a suitable admittance value for the resonator. This can be achieved by properly fixing the ratio (W/d_v). In order to obtain a compact structure, the minimum practical value for the inner via diameter is chosen. Next, the loading capacitance is adjusted by means of the metal patch perimeter or the width of the isolating gap s_p, although normally the width of the latter is also fixed to the maximum resolution of the manufacturing process (i.e., typically about 100 – 200 μm for standard PCB technology) for increasing the capacitive effect.

Input/output coupling to the resonator is usually performed using a modified coplanar waveguide (CPW) probe, which enables the use of thick substrates. This probe is typically composed of a coplanar-to-microstrip transition short-circuited to the SIW top ground plane. Slots can be added at the end of the microstrip in order to control the coupling level.

Ultimately, the unloaded Q that can be achieved in this structure is close to the one obtained in conventional SIW resonators [25], with additional conductor losses coming from the inner conductor. Thus, an unloaded Q-factor of 200 – 300 can be easily obtained with low-cost hydrocarbon ceramic materials.

Coaxial SIW Bandpass Filters

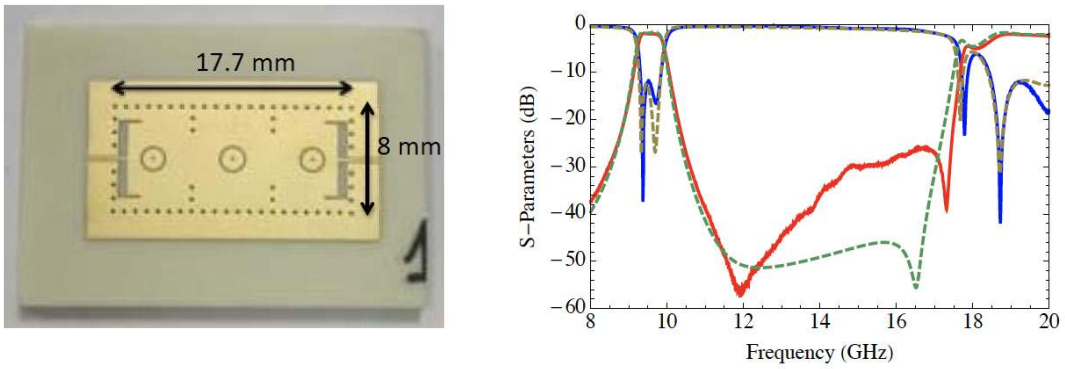

(a) (b)

Figure 2. (a) Photography of a 3-pole in-line bandpass filter at 9.8 GHz with magnetic-field coupling between resonators using inductive irises, and (b) measured S21 (solid red) and S11 (solid blue) parameters of the device compared with full-wave EM simulations (dashed) [25].

Bandpass filters based on coaxial SIW resonators can be implemented by coupling several cascaded resonators. In line bandpass filters implementing all-pole responses can be realized by using inductive irises between adjacent resonators for controlling the magnetic coupling level as in [25], where a 3-pole 5% fractional bandwidth (FBW) Chebyshev filter at 9.8 GHz was designed and manufactured. In the example shown in Fig. 2(a), the device footprint is 3 times smaller than that of a conventional SIW implementation. Thus, this approach enables the design of very compact narrow band filters with enhanced spurious-free bands due to the smaller resonator length, as can be

seen from the response in Fig. 2(b). An estimated unloaded Q-factor of about 170 can be extracted from the experimental results.

Both positive and negative coupling networks, as well as coupling mechanisms between non-adjacent resonators, are usually required for the introduction of finite transmission zeros (TZs) due to signal cancellation. Even if non-adjacent resonators can be coupled by means of folded topologies, there is no straightforward way in conventional SIW technology to obtain both coupling signs. The first approach reported in the literature consisted of a balanced microstrip line with plated via holes for phase inversion [35]. However, this requires etching the bottom ground plane which reduces the ease of integration and stand-alone nature of the filter. Later, other solutions based on grounded coplanar lines [36], mixed-couplings [37], [38], and over-moded cavities [39] were proposed, although they typically introduce some limitations in terms of coupling level, topology, or area required.

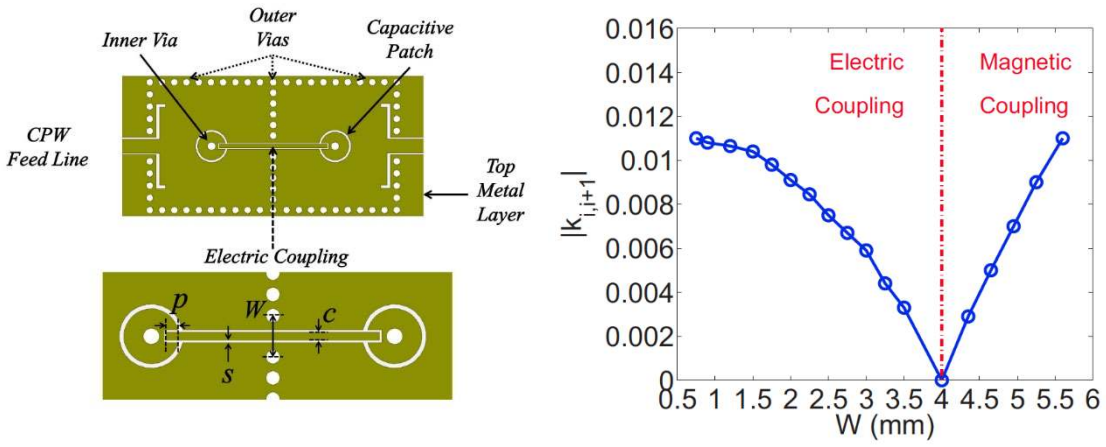

(a) (b)

Figure 3. (a) Layout of the electric-field coupling probe for coaxial SIW resonators and (b) coupling coefficient variation versus the width of the iris window *W* for a given probe dimensions and penetration into the capacitive patch [40].

However, negative (or electric) coupling in coaxial SIWs can be achieved in a single-layer technology due to the direct access to the capacitive section of the resonator. Thus, a single open-circuited coplanar probe can be used for introducing electric-field coupling between resonators. Different parameters can be used for controlling the coupling level, such as the penetration depth into the capacitive metal patch, the probe dimensions, or the width of the inductive iris between cavities (i.e., by modifying the intrinsic magnetic-field coupling between resonators and hence counteracting the electric contribution). A schematic of the electric-field coupling probe for a coaxial SIW is shown in Fig. 3(a). As can be seen, the sign of the coupling can be reversed by decreasing the magnetic-field coupling contribution introduced by the inductive iris between resonators, as depicted in Fig. 3(b). This approach was extensively studied in [40] and employed for designing in line filters with electric-field coupling [40] and pseudo-elliptic filters [41], as well as diplexers [27].

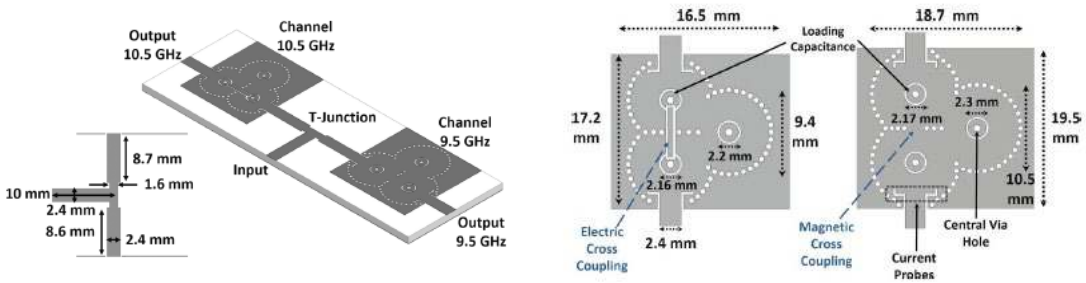

(a) (b)

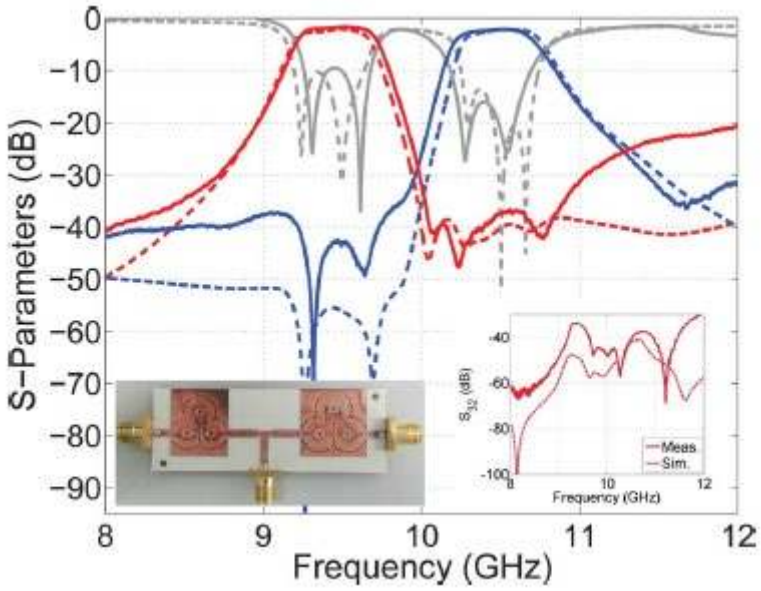

(c)

Figure 4. (a) Geometry of the proposed diplexer, (b) detailed view of the channel filters with negative (left) and positive (right) cross-couplings, and (c) measured (solid) and simulated (dashed) results [27].

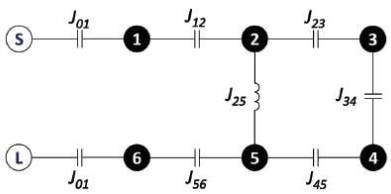

(a)

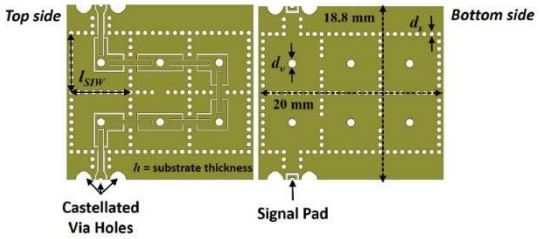

(b)

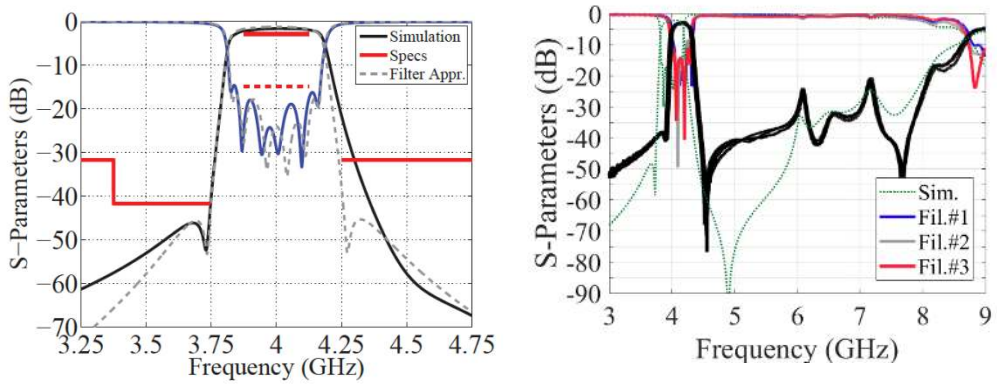

(c) (d)

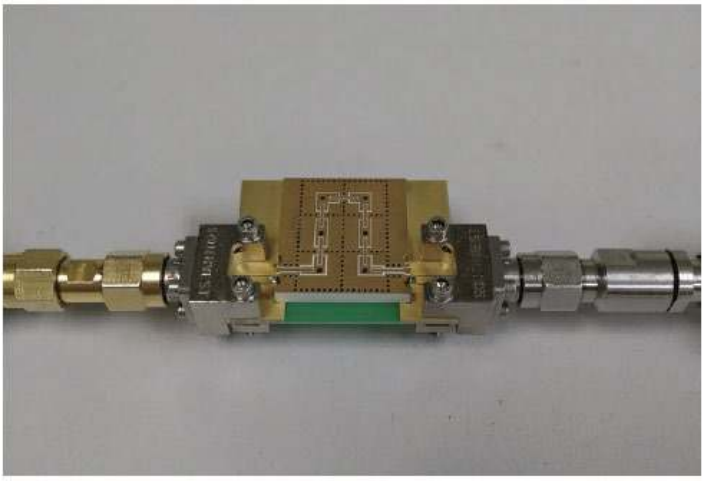

(e)

Figure 5. (a) Filter topology, (b) device structure, (c) synthesis and EM simulation results, (d) measured results for three different devices showing good repeatability, and (e) photograph of the manufactured device under measurement [31].

For instance, an X-band diplexer was designed and manufactured in [27] with TZs placed below and above each passband in order to improve rejection and isolation levels. A schematic of the proposed design, as well as the layout and measured results, are shown in Fig. 4. The device was manufactured in 1.52 mm-thick RO4003C. The entire device dimensions are 58.4 x 18.7 mm^2 excluding I/O feeding lines. Maximum insertion losses

of 1.6 dB and 2.1 dB are obtained at the lower and upper channels respectively, while stopband suppression is better than 37.5 dB at both bands. An unloaded Q-factor of 180 was extracted from the measured results.

In order to achieve filter miniaturization, thick ceramic-filled PCB substrates with high permittivity values can be employed. In this way, the impedance of the resonator is reduced, and the capacitive loading increased by means of metal patches with greater perimeter. Following this approach, a 6^{th}-order filter with two TZs was presented in [31]. The topology of the filter and a schematic of the device are shown in Fig. 5(a) and (b). Electric-field coupling is used for input/output and direct-coupled resonators, while inductive irises are used for introducing a cross-coupling between resonators 2 and 5, thus producing a pseudo-elliptic response [26]. A 2.54 mm-thick Rogers TMM10i substrate (ε_r=9.8, $\tan\delta=2\cdot10^{-3}$) was chosen for implementing the device. The filter included vertical CPW-to-CPW transitions for enabling SMD packaging of the structure and assembly on top of a carrier substrate. The footprint was just 20 x 18.8 mm^2, showing a high degree of miniaturization at C-band (i.e., 75% reduction in area with respect to an equivalent TE_{101}-based SIW implementation).

While the design and optimization process resulted in a very satisfactory design, as can be seen in Fig. 5(c), the measured results revealed a small shift towards higher frequencies, due to the trapezoidal shape of the gaps etched on the top substrate, which slightly reduces the effective loading capacitance. However, the repeatability within the same lot is very good, as can be seen from Fig. 5(d). An unloaded Q-factor of 180 was extracted from the measurements. A higher insertion loss level was obtained compared to simulations, with an expected unloaded Q of 240. This effect can be attributed to the

additional losses produced by the electroless nickel immersion gold finishing covering the bare copper surface. A photograph of the manufactured filter under measurement is shown in Fig. 5(e).

In Table 1, the main parameters of the coaxial SIW bandpass filters described above are summarized. Recently, other examples of very compact coaxial SIW filters have been presented. For instance, a compact quasi-elliptic combline filter in single-layer SIW technology using mixed coupling schemes was presented in [42]. Other approaches rely on multi-layer PCB technology for embedding the capacitive post in one of the inner substrate layers, thus enabling a huge increase in the loading capacitance and therefore producing very compact implementations [43]. A similar concept can be further exploited in low temperature co-fired ceramic (LTCC) technology for achieving miniaturization factors close to 97% [19], [44].

Although extreme miniaturization can be obtained at UHF and in the S-band by increasing the loading capacitance using lumped capacitors, thus lowering the resonant frequency of the resonator, special care must be taken with the out-of-band response as the higher-order modes usually shift to lower frequencies. Multi-layer implementations with buried post capacitance axially loaded with surface mount capacitors have demonstrated a high level of miniaturization with a wider stop-band compared to single-layer implementations [45].

Table 1 A comparison of the coaxial SIW bandpass filters described in this review.

Ref.	f0	BW	Order	TZ	IL	Size
[25]	9.8 GHz	5%	3	No	1.7 dB	$0.58\lambda_0$ x $0.26\lambda_0$ x $0.050\lambda_0$
[27]	9.5 GHz 10.5 GHz	4.2% 3.8%	3 3	1 1	1.6 dB 2.1 dB	$2.04\lambda_0$ x $0.65\lambda_0$ x $0.053\lambda_0$ *Diplexer including T-junction*
[31]	4 GHz	7.5%	6	2	2.8 dB	$0.27\lambda_0$ x $0.25\lambda_0$ x $0.034\lambda_0$

Flexible and Advanced Filtering Responses

Singlets and Cascaded Singlets

The selectivity provided by a filter in the vicinity of the passband can be improved by generating TZs rather than by increasing the number of its poles [46]. The idea of exploiting additional signal paths between the source-load and resonators is not new, but it is very useful for microwave filter designers [47], [48], [49]. The most common approach to generating TZs is to arrange the resonators in such a way that cross-coupling mechanisms among resonators can be created, leading to signal cancellations at the output, as discussed in the previous section. This strategy can produce *N* TZs with *N* resonant elements if there is also input-output coupling (otherwise, the maximum number of TZs is *N-2*). An alternative method of TZ generation is to add additional paths that bypass the resonant element itself, which allows the design of advanced filtering responses that have *N* TZs. To do that, several singlets (i.e., the most basic building blocks that contain one resonator and generate one TZ, fist defined in [50]) must be cascaded using non-resonating nodes (NRN) to attain the modular design of such elliptic filters.

The routing scheme of a singlet is depicted in Fig. 6(a), which shows the single resonator with the input/output couplings m_{s1} and the source/load coupling m_{sl}. This topology can be designed in coaxial SIW technology by means of a direct source-load coupling that can be implemented at the top layer. Furthermore, this scheme in coaxial SIW enables simple realizations of different coupling signs, which are needed for the flexible positioning of the TZ.

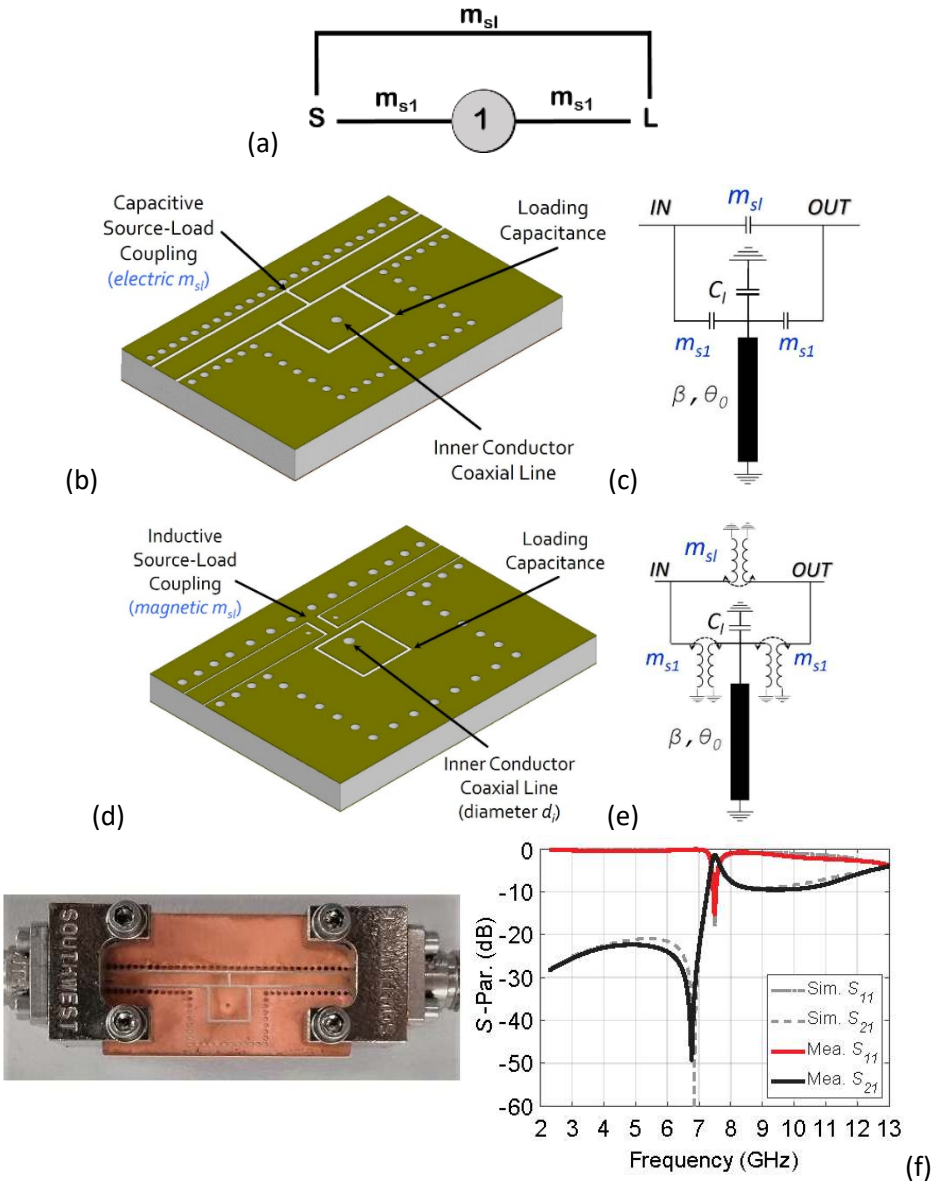

Figure 6: (a) Routing scheme of a singlet. (b) Coaxial SIW singlet with TZ below the passband with (c) its equivalent circuit. (d) Coaxial SIW singlet with TZ above the passband with (e) its equivalent circuit [52]. (f) Practical realization of a singlet in coaxial SIW topology with TZ below the passband [51].

Thus, a fully integrated technique for the design of a coaxial SIW singlet was successfully proven in [51] using a direct electric source-load coupling m_{sl}, which is based on a distributed series capacitance created on the CPW feeding line. The TZ in this singlet is generated below the passband, and its position is set by the spacing and width of the gap that establishes this capacitance. Fig. 6(b) and(c) show the layout of such a coaxial

SIW singlet and its equivalent circuit, respectively. In addition, Fig. 6(f) depicts a practical implementation of a coaxial SIW singlet centered at 7.5 GHz with a TZ located at 6.8 GHz.

An evolution of this coaxial SIW singlet was then proposed in [52], so that the TZ could be generated above the passband. In this case, the m_{sl} is based on a magnetic-field coupling mechanism, which has been obtained by means of a standard CPW-to-SIW transition that makes use of a current probe (i.e., a plated via hole is inserted at the end of the CPW feeding line) as shown in Fig. 6(d). The equivalent circuit is also depicted in Fig. 6(e).

The various coaxial SIW singlets can be used as building blocks of bandpass filters with symmetric quasi-elliptic response, or asymmetric responses with steep filter skirts. Once the singlets have been designed, they can be coupled among them by means of the quarter-wave coplanar waveguide (CPW) NRNs, whose resonant frequencies should be quite different from the desired working frequency.

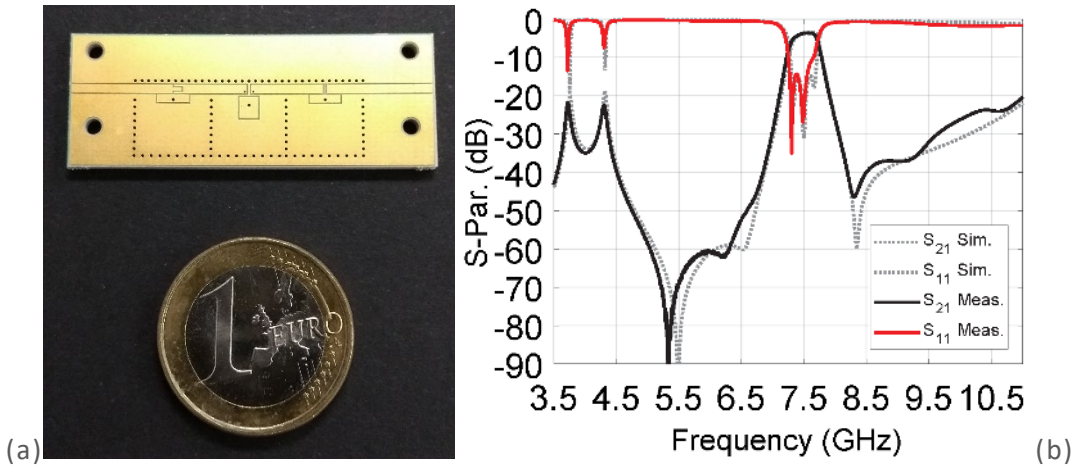

Figure 7: Three-pole elliptic BPF based on three cascaded singlets: (a) photograph, and (b) measured and simulated responses.

Fig. 7 shows the performance of a third-order elliptic filter, showing two TZs below, and one TZ above, the passband, which fully benefits from the design flexibility offered by these building blocks. Fabricated using a 1.52 mm-thick Rogers R4003C, this BPF was designed by cascading three singlets with different source-load coupling schemes. Specifically, two singlets show electric bypass coupling (i.e., the first and the third resonators responsible for lower TZs), while the second one has a magnetic bypass coupling, which generates the upper TZ. The filter's center frequency is 7.5 GHz, while the FBW measured at the level of RL = 15 dB is 5% (i.e., BW = 380 MHz). The filter rejection is extremely good (between 4.5 GHz and 6.7 GHz, which is better than 48 dB), while its size of 9.8 × 28.5 mm^2 enables a 50% reduction in area with respect to an equivalent TE_{101}-based SIW implementation.

Dual-mode Coaxial SIW

Like its equivalent waveguide counterpart, the coaxial SIW topology is able to support two propagation modes [53], [54], thanks to its very flexible 2.5D geometry that enables the introduction of two (or more) conducting posts connected to their own patches in the very same SIW cavity resonator. Fig. 8 shows the layout of a dual-mode coaxial SIW cavity, a cross-sectional view, and the corresponding equivalent circuit [53], [54].

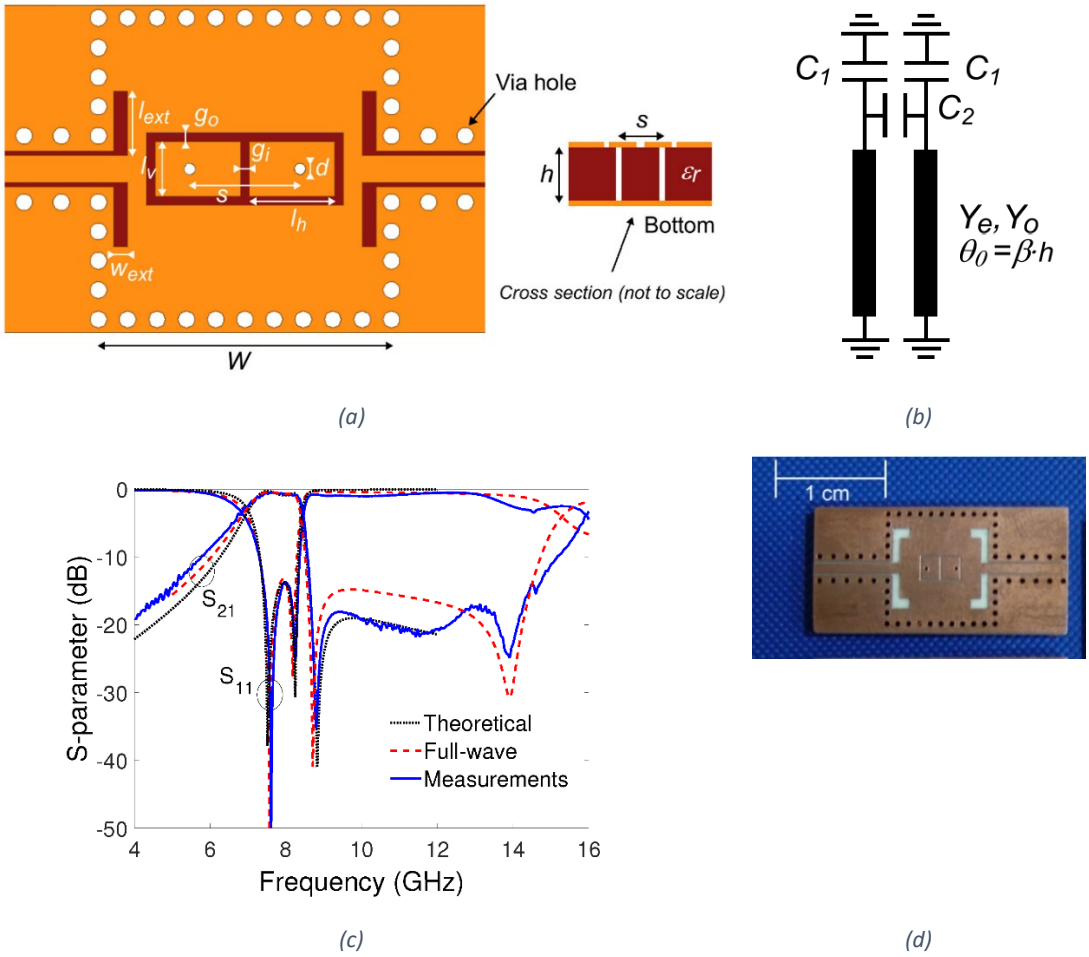

Figure 8: (a) Layout of a dual-mode coaxial SIW resonator, (b) equivalent model, (c) theoretical, 3D EM simulated and measured responses of the implemented filter and (d) photograph of the fabricated device [54].

On the one hand, two via holes are symmetrically inserted with respect to the SIW cavity center, and they are then connected to separate capacitive patches at the top layer. On the other hand, at the bottom layer, there is no difference from a standard coaxial SIW, where those via holes are short-circuited to ground. Such dual-mode configuration has the clear advantage of enabling a sharp improvement of the achievable BW, out-of-band rejection, and compactness. Since there are two separate coupling paths between the source and the load in a doublet configuration, this topology features one TZ in the frequency response.

This simple topology offers the flexibility of designing both narrowband and wideband compact filters with improved rejection that provides a high degree of flexibility. To corroborate the usefulness of this topology, two filters exhibiting wide- and narrow-band responses were designed, fabricated, and measured [54]. Fig. 8 shows the layout of the wideband BPF with a center frequency f_0 = 8 GHz and FBW_{3dB} = 20%, and a photograph that shows a square SIW cavity size of 10.6 mm. Despite the fact that a single-layer PCB was used, the designed dual-mode filters enable a 75% reduction in area, compared to a standard SIW filter implementation. The reduction in area might be stretched up to 90% with a proper resonator design. The stopband of the filter is spurious-free up to 14.6 GHz, which is around $2\times f_0$, where the SIW cavity TE_{101} mode is excited.

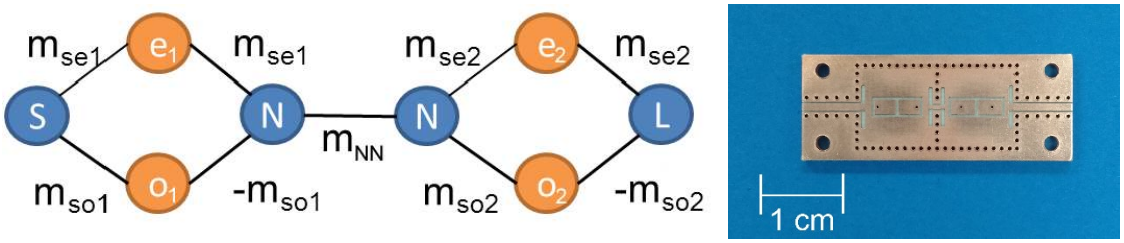

(a) (b)

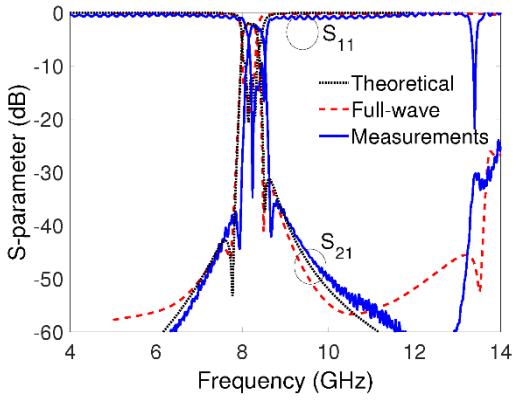

(c)

Figure 9: A 4-pole quasi-elliptic type BPF created by cascading two dual-mode SIW coaxial cavities. (a) Routing coupling scheme and photograph. (b) Theoretical, full-wave simulated, and measured responses of the fabricated BPF [53].

Cascading dual-mode building blocks by means of NRNs is a straightforward way to implement complex filtering responses with high-selectivity performance and multiple TZs. For instance, Fig. 9 shows the layout of a 4^{th}-order narrow band BPF with FBW_{3dB} = 4%, which presents a quasi-elliptic type response, since two TZs are generated above and below the passband. Note that in Fig. 9, e_i and o_i indicate the even- and odd-mode resonator node, respectively, whereas $m_{se,i}$ and $m_{so,i}$ are the main direct couplings to the even- and odd-mode, respectively. A clear advantage of this approach is that each doublet can be designed individually.

This promising approach can be further developed to design dual band filters that feature two independently controllable bandwidths in a single SIW cavity resonator [52], as shown in Fig. 10, which achieves a dramatic improvement in the component miniaturization. Indeed, the proposed doublet configuration with electric-based direct bypass coupling was employed to design two dual band filters with TZs at both sides of the passbands (i.e., four TZs placed at real frequencies), and with different bandwidth requirements (see details in [52]). A very interesting property is that both passbands can be independently controlled, since there is no coupling between the upper and lower side of the cavity. The filter shown in Fig. 10, (labeled as DB2 in [52]), operates at 5.25 GHz and 7.5 GHz, providing FBW_{1dB} = 12.8% (i.e., BW = 670 MHz) and FBW_{1dB} = 2.7% (i.e., BW = 200 MHz), respectively.

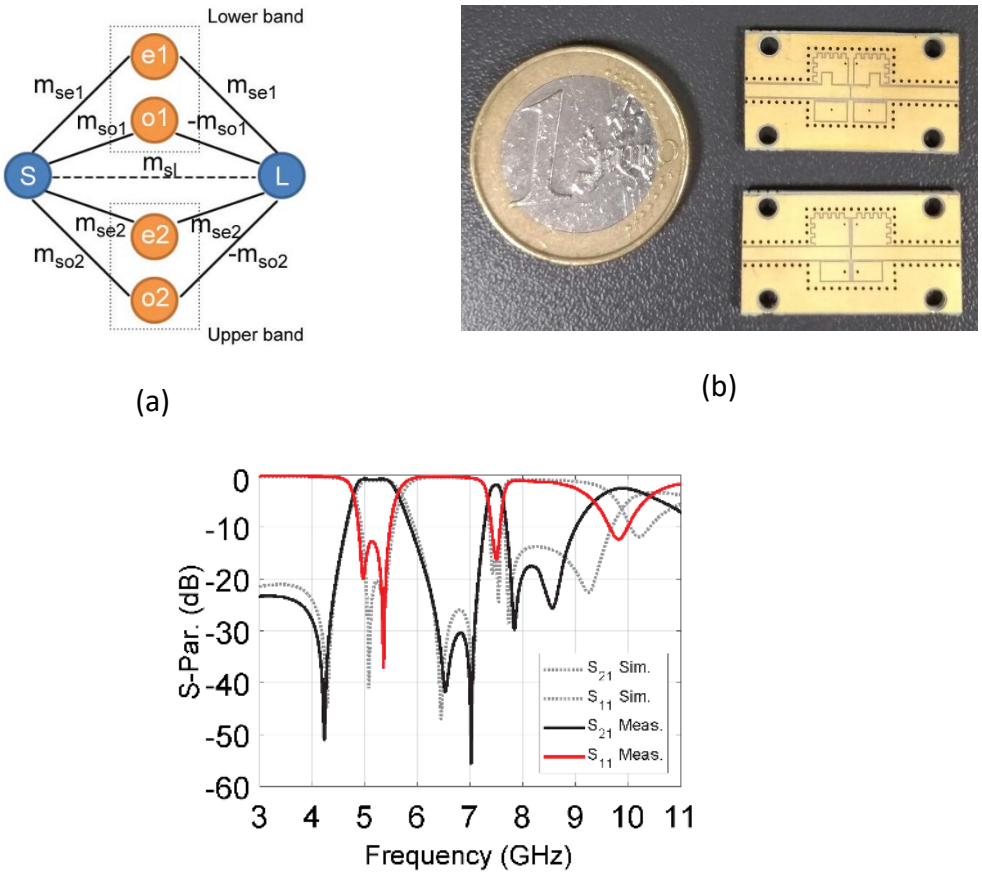

Figure 10: (a) Routing coupling scheme of the proposed dual-band filter based on a coaxial SIW doublet. (b) Photograph of two filter prototypes (the one shown below is labeled as DB1, the other as DB2) with different passband configurations, and (c) the measured response of the filter DB2 [52].

Tunable Coaxial SIW Filters

The availability of moderate-to-high *Q*-factor tunable resonators (i.e., with unloaded Q-factors higher than 100) is of primary concern in the design of low-loss reconfigurable filters for microwave applications, since they are going to be of enormous importance in the development of future multi-band multi-standard miniaturized front-ends, for both satellite and terrestrial applications. Nevertheless, it is difficult to find an acceptable compromise among fast tuning speed, low loss, wide tuning range, compact size, low manufacturing cost, and reliability, which are very important characteristics to

offer in most applications. Likewise, to increase the transceiver reconfigurability, these devices must also offer bandwidth tuning, which is a non-trivial feature to be addressed.

When implementing frequency-agility in SIW components, the main advantage of the coaxial SIW topology stems from the fact that the integrated loading capacitance is readily accessible at the top metal layer. This means that the frequency tuning can be achieved simply by assembling suitable tuning elements that are called upon to modulate such loading capacitance. This tuning procedure can be classified into two categories depending on the way in which the resonant frequency is changed: analog and discrete tuning. Both mechanisms have been widely demonstrated in the literature to be seamlessly applicable to coaxial SIW topology.

The first example of a tunable coaxial SIW structure was proposed in [55]. Specifically, a continuously tunable coaxial SIW resonator, which made use of a GaAs varactor diode MA46H200 from MACOM, was designed for working at the S-band between 2 and 3 GHz, the simple layout of which is shown in Fig. 11.

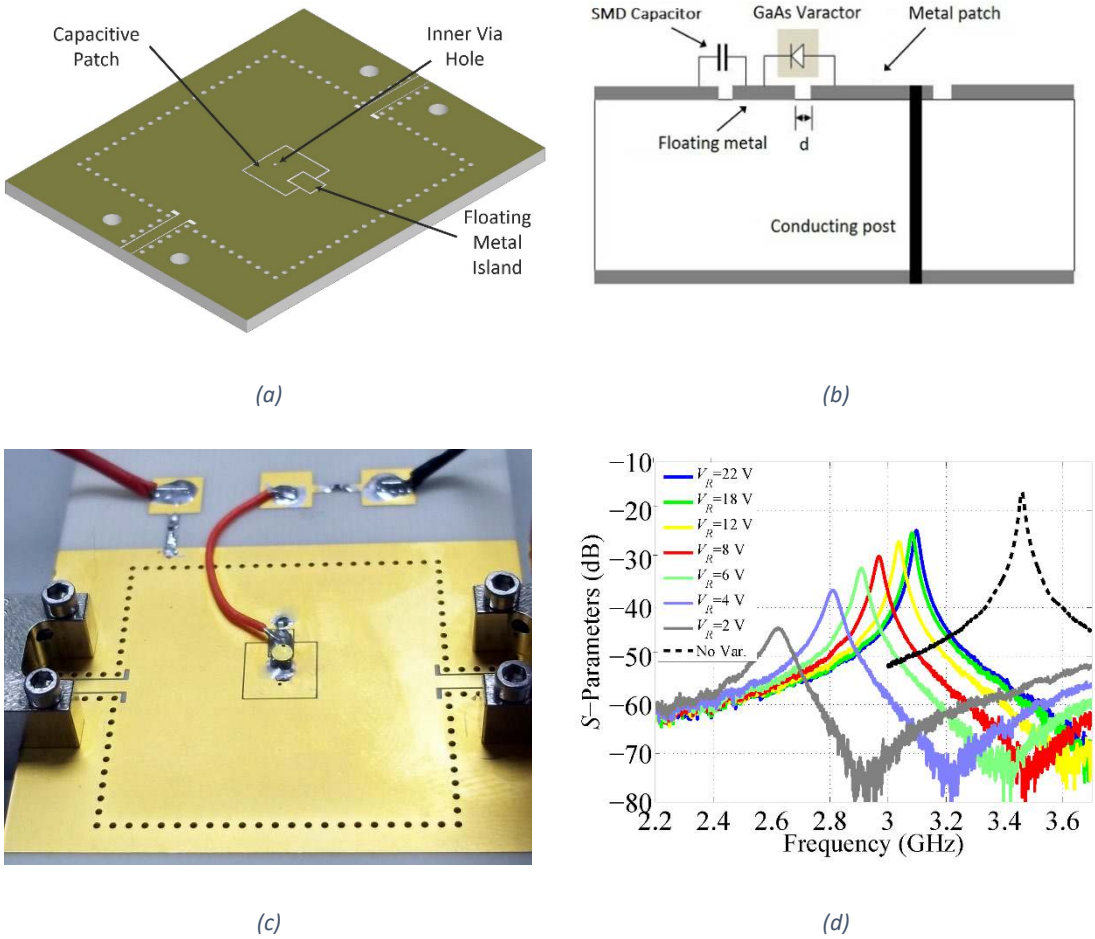

Figure 11: (a) S-band varactor-tuned coaxial SIW resonator, (b) its cross-sectional view, (c) manufactured tunable resonator, and (d) measured results (only the S21 parameter is shown) [55]. The resonator size is 27 x 27 mm² with a 6.2 x 6.2 mm² capacitive patch with a 0.1 mm isolating gap. Via hole and conductive post diameters are 0.5 mm and 0.3 mm, respectively.

A floating metal patch needs to be introduced between the capacitive patch and the SIW ground plane, and be completely isolated from them, in order to allow for the assembly and biasing of the varactor diode, as can be seen in Fig. 11(a) and (b). A fixed SMD capacitor is then inserted in series between the floating metal and ground to increase the tuning range (which would be reduced by the small capacitance generated by the floating metal air gap).

Fig. 11(c) shows a photograph of the tunable resonator prototype, and the measured results are depicted in Fig. 11(d). The varactor-tuned resonator shows a wide tuning

range of almost 20%, between 2.64 GHz and 3.1 GHz (for reverse bias voltage V_b 2-22 V). In addition, the extracted Q_u ranges from 40 at 2.64 GHz to 160 at 3.1 GHz, while the static resonator presents a Q_u of 220.

This structure has been successfully exploited for the design of reconfigurable filters, for example in [56], where a 2-pole bandpass filter was designed. However, the major drawback of this preliminary filter was the variation of its FBW along the tuning range, specifically, from 5% at 2.88 GHz to 2.3% at 2.5 GHz. This issue is due to the short resonator electric length ($\theta_0 = 11°$) that provokes a wide variation in the coupling coefficients over frequency.

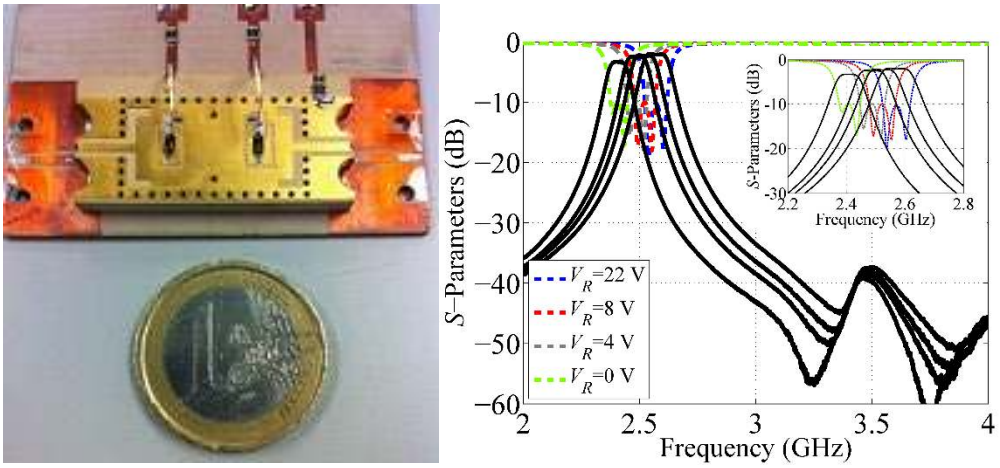

Figure 12: (a) The manufactured 2-pole varactor tunable filter and (b) its measured results [59].

To overcome this BW variation, the use of tunable coupling mechanisms is needed, which are based on variable reactive elements [17], [57]. However, as demonstrated in [58], proper selection of the resonator length can help to reduce the variation in the inverter values and keep a constant fractional bandwidth. To do that, thicker substrates must be chosen for implementing longer coaxial SIW resonators, as in [59].

Fig. 12 shows a photograph and measurements of a 2-pole tunable filter designed to work in the S-band, which has been implemented in a 3.81 mm-thick laminate of Rogers TMM10i substrate (ε_r = 9.8 and tanδ = 0.002) and which size is just 16.5 × 33 mm^2. Measurements show a continuous tuning from 2.4 GHz (IL = 3.4 dB) to 2.6 GHz (IL = 1.9 dB) with FBW_{1dB} (from 3.9% at 2.6 GHz to 3.3% at 2.4 GHz) and almost constant return losses (RLs). Good rejection was obtained using the same tuning mechanism described above. Moreover, the Q_u is estimated to be 145 @ 2.6 GHz and 110 @ 2.4 GHz, which is higher than 100 in the whole tuning range.

In addition, the use of tunable couplings in reconfigurable coaxial SIW filters allows designers to achieve extremely high levels of response reconfiguration. Such an approach has been reported in [60] and [61]. Using as a building block the varactor tunable resonator previously described, mixed inter-resonators and external coupling mechanisms are employed to implement bandwidth tuning. On the one hand, the primary dominant coupling path is between the magnetic fields created by the two closely placed inner posts of adjacent resonators, with a fixed amount of coupling. On the other hand, a weaker secondary path is generated through the electric fields created by lumped varactors that directly connect the capacitive patches of adjacent resonators as well as the feeding lines (see Fig. 13(a)-(b)). Here, low-*Q* tuning elements can be used to tune the BW without significantly affecting the resonator Q_u. Then, to increase the tuning range, several varactor diodes in back-to-back configuration are assembled on the resonator capacitive patch [33], [62]. The huge loading effect enables further miniaturization of the filter, which operates in UHF and the L-band showing measured resonator Q_u in the range of 100-200 with off-the-shelf varactor diodes.

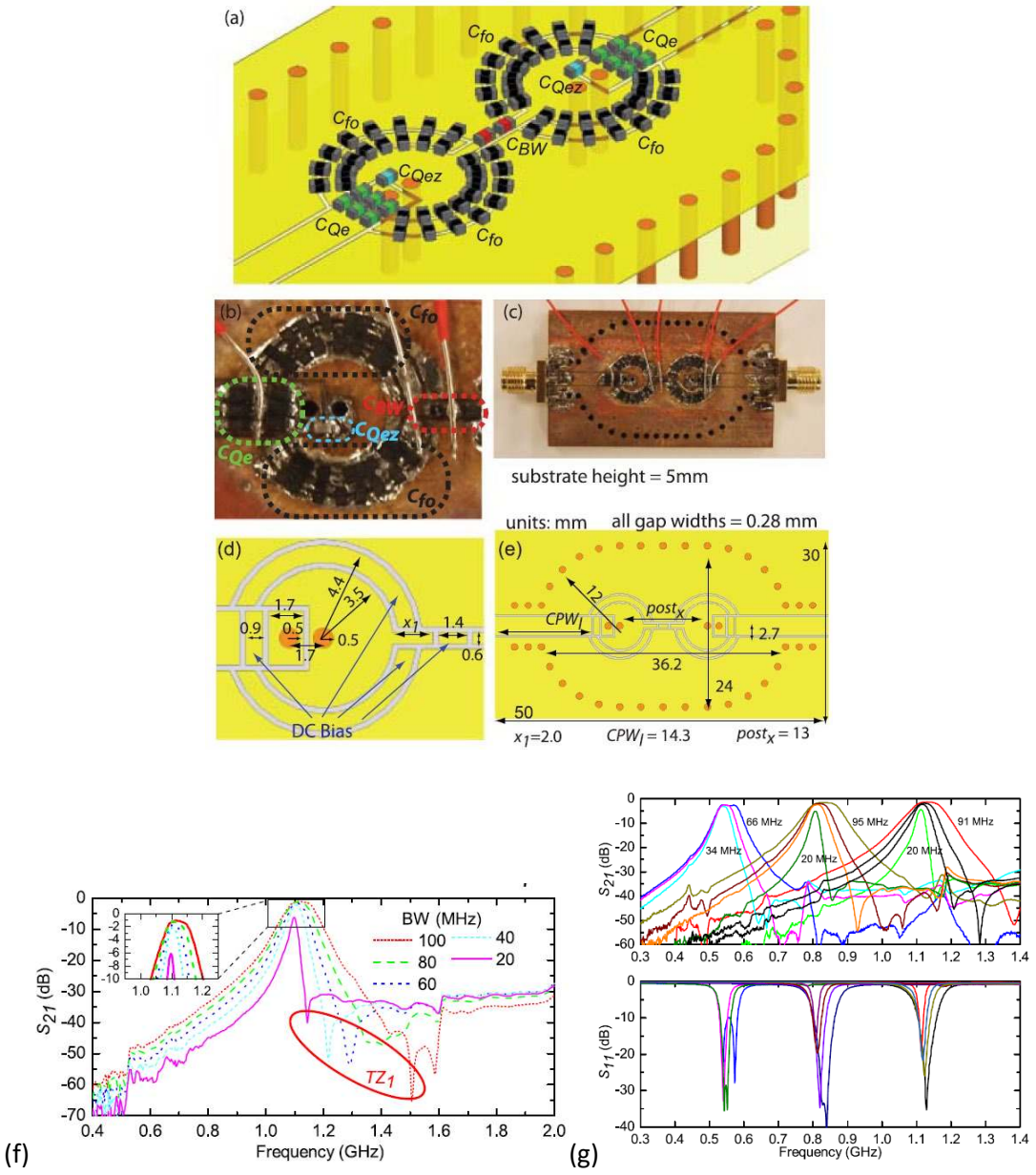

Figure 13: (a) Designed coaxial SIW filter with two ring gaps and back-to-back varactors, (b) close-up and (c) full-view of the fabricated filter, (d)-(e) dimensions of the filter, (f) measured S_{21} showing decreasing BW as the varactor capacitance increases, and (g) measured S21 and S11 for both tunable center frequency and BW [61].

Fig. 13(f) and (g) shows the remarkable results that such a filter implementation with tunable center frequency and BW can achieve. In particular, the FBW can be controlled as follows: 6.18%–12% at 0.55 GHz, 2.38%–11.3% at 0.84 GHz, and 1.77%–8.05% at 1.1 GHz. The extracted Q_u for the resonators is approximately 80 at 0.5 GHz and 200 at

1.1 GHz. Furthermore, this varactor tunable filter can show a constant BW anywhere from 34 to 66 MHz along the whole tuning range.

Today, tunable dual-mode coaxial SIW resonators have emerged as a very attractive building block of reconfigurable filters, as they enable the realization of a wide variety of filtering responses while maintaining an extremely compact size and planar integration. One especially desirable feature of these resonators is the ability to control the resonant frequency of each mode independently, while generating one TZ in the frequency response [63], [64], [65].

Indeed, in [63], two vertically moving tuners enabling independent tuning for each mode of a dual-mode SIW resonator have allowed the design of a high-Q, widely tunable second-order BPF. The layout and a photograph of the tunable filter prototype are shown in Fig. 14. In addition to the wide tuning range, this doublet configuration permits flexible control of the TZ on the lower or the upper side of the passband.

To enable this tuning, two flat tuners with conductive surfaces are positioned on top of the resonator, creating two different controllable gaps (g_1, g_2) with the primary role of modifying the embedded capacitances [C_1 and C_2 shown in Fig. 14(c)] that belong to the dual-mode resonator. The filter was designed on a 5.08 mm-thick Rogers TMM3 substrate, whereas the tuners are cut from a 0.75 mm-thick Rogers 4003 substrate, and attached to an M3L linear actuator in order to create the vertical motion. The measured results are very good, with a wide tuning range (2 GHz-3.2 GHz), and a high Q_u that is better than 200 between 1.7 GHz and 3 GHz.

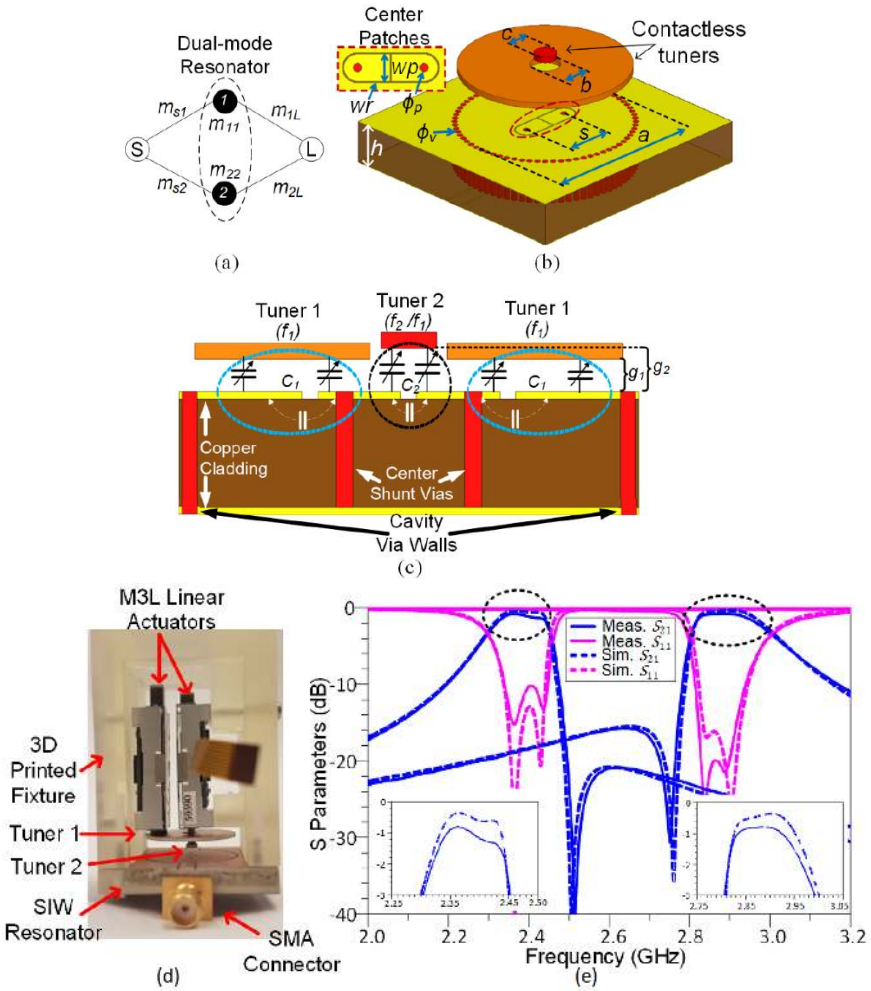

Figure 14: (a) General coupling diagram with a dual-mode resonator. (b) Proposed dual-mode SIW resonator. (c) Cross-section of proposed resonator. (d) Picture of fabricated filter with fixture and M3L linear actuators. (e) Measurement and simulation comparison for two tuning states [63].

However, this approach has the disadvantage of needing a more complex tuning structure, resulting in a bulky filter implementation. At the expense of poorer *Q* performance (i.e., in the range 50-150), this promising tunable doublet topology can also be deployed using SMD varactor diodes [64], or using manually adjustable thin-film trimmer capacitors [65].

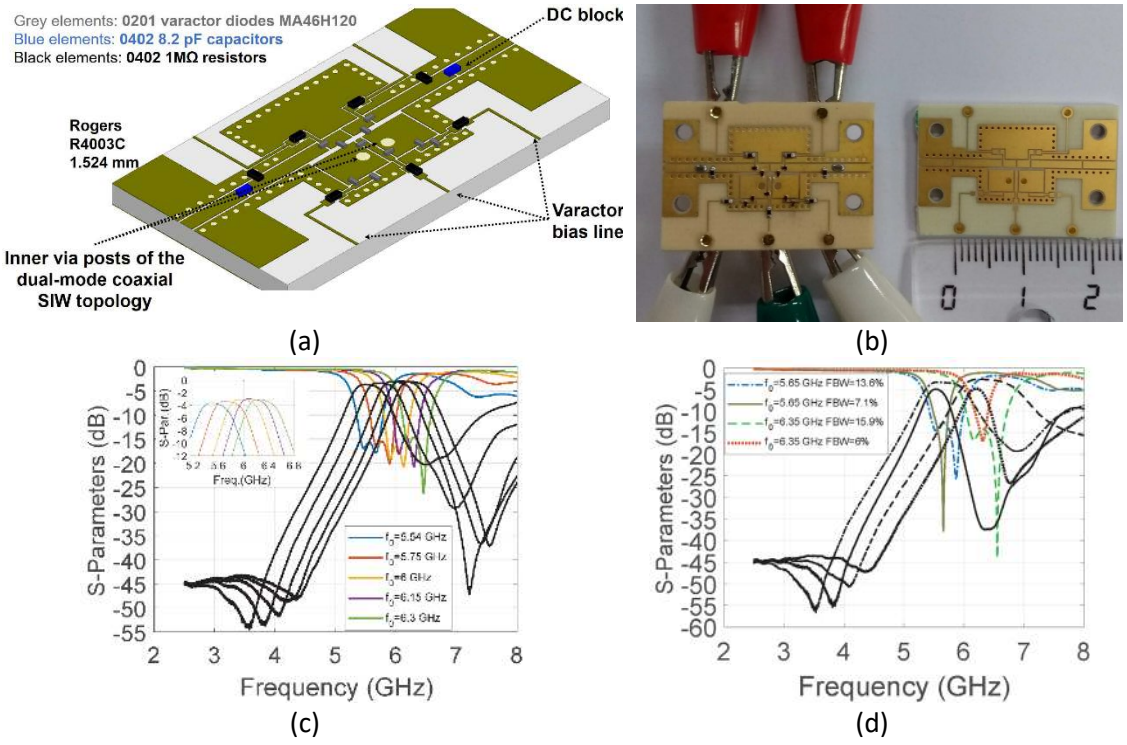

Figure 15: (a) Tunable doublet layout with SMD components, (b) a photograph of some filter prototypes, (c) measured frequency responses with constant BW3dB = 600 MHz. and (d) measured frequency responses when both BW and f_0 are controlled simultaneously [64].

Indeed, in [64], flip-chip varactor diodes are used as tuning elements for the frequency- and bandwidth-tuning of a C-band coaxial SIW doublet, which is also able to show two TZs at both sides of the passband thanks to a direct source-load bypass coupling. As can be seen in Fig. 15, the filter keeps a full planar integration since both SMD footprint pads and biasing lines have been embedded in the very same substrate, which means that this tunable device requires just a low-cost single-layer PCB and standard SMD assembly.

The measured results shown in Fig. 15(c)-(d) exhibit an improved filter response flexibility that allows the filtering responses to have either constant absolute BW or

adjustable BW over a 13% tuning range at the C-band. Specifically, the insertion loss and return loss are always better than 5 dB (i.e., Q_u between 60 and 100, which is an appealing range considering the working frequency band) and 15 dB, respectively, over the whole tuning range. Finally, the filter is tuned from 5.65 GHz to 6.35 GHz with an FBW range of 6%-15.9% at 6.35 GHz and 7.1%-13.6% at 5.65 GHz.

A further development of the dual-mode topology includes loading an SIW cavity with four identical metallic posts, giving rise to two degenerate modes. Loading the ends of the inner posts with variable-reactance elements allows these modes to be exploited to design quasi-elliptic-type filtering transfer functions with multiple levels of spectral adaptivity, which includes center-frequency control, bandwidth tuning, and intrinsic RF switching-off [65]. To improve overall performance, high-Q manually adjustable thin-film trimmer capacitors are used. As a result, the four-pole/four-TZ filter shown in Fig. 16 exhibits center-frequency reconfigurability in the range of 1.7-2.5 GHz and BW tunability between 58 MHz and 156 MHz, achieving a Q_u that is in the range of 120-150. The intrinsic switching-off mode presents a measured maximum in-band attenuation of 38 dB and a minimum in-band attenuation of 21.5 dB within the range of 1.91-2.1 GHz.

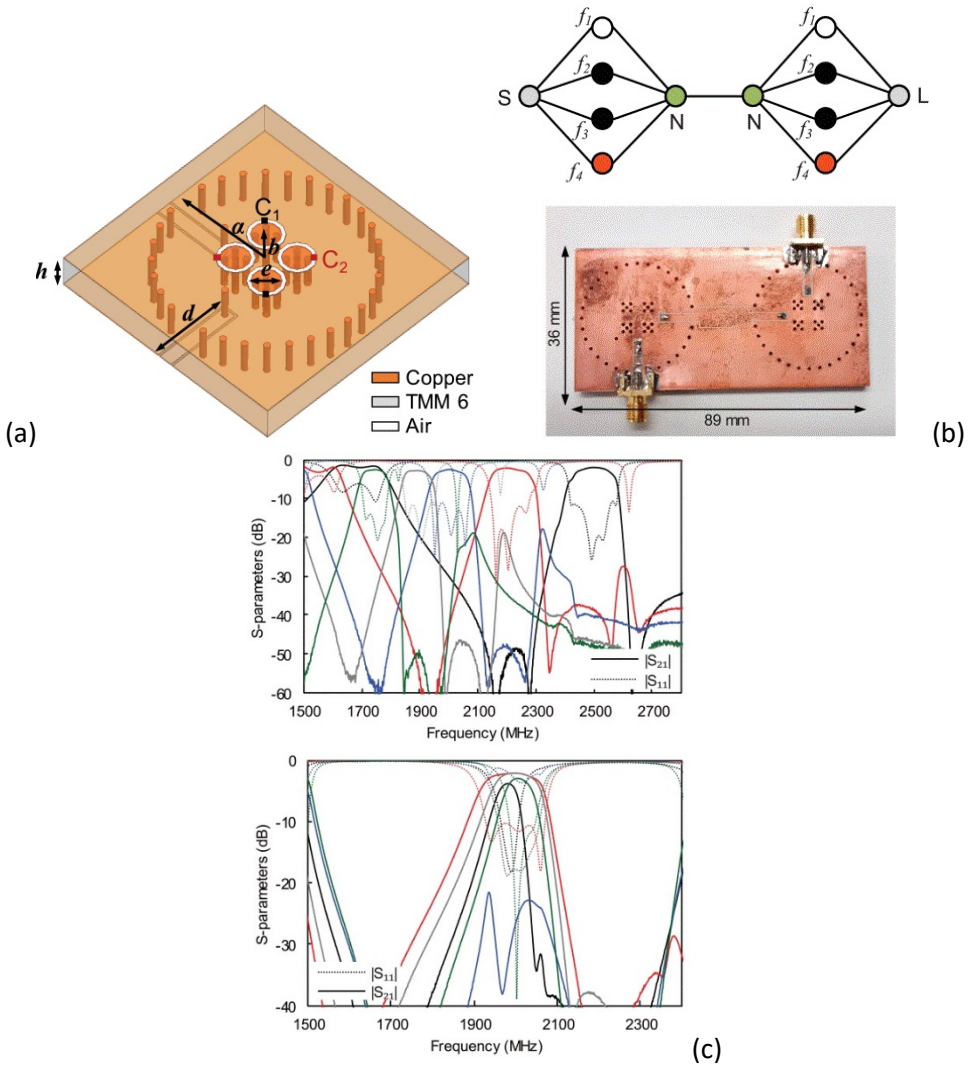

Figure 16: (a) Three-dimensional model of the dual-mode SIW-cavity-based BPF single-section. Four-pole/four-TZ bandpass filter prototype: (b) coupling-routing diagram (green circles: non-resonating nodes; gray circles: unitary source and load; black, white, and red circles: resonating modes; and black lines: couplings) and manufactured prototype, (c) measured S21 and S11 responses of the two-section dual-mode SIW-cavity-based bandpass filter in terms of center-frequency and BW tuning, including intrinsic switch-off [65].

Finally, it is evident that a simple digital tuning based on switchable planar capacitances can also be applied to the coaxial SIW topology. Despite the demonstrated improvement in the overall *Q*-factor enabled by this approach, just a few examples of digitally tunable coaxial SIW filters have been proposed thus far [66], [67], [68]; these filters show tuning ranges between 15% and 20%, with Q_u easily higher than 100 at C-band working frequencies.

This straightforward method for obtaining digital frequency control is based on the introduction of embedded tuning capacitances on the loading capacitive patch of a resonator by creating electrically isolated elements. Then, PIN diodes as well as RF MEMS resistive switches are assembled between the integrated capacitors in order to achieve switching operability. Apart from the improvement in Q_u, such tuning capacitance integration has several advantages in terms of limited BW variation versus frequency, higher tuning range, and flexible positioning of the frequency states by separately adjusting the size of each tuning capacitance.

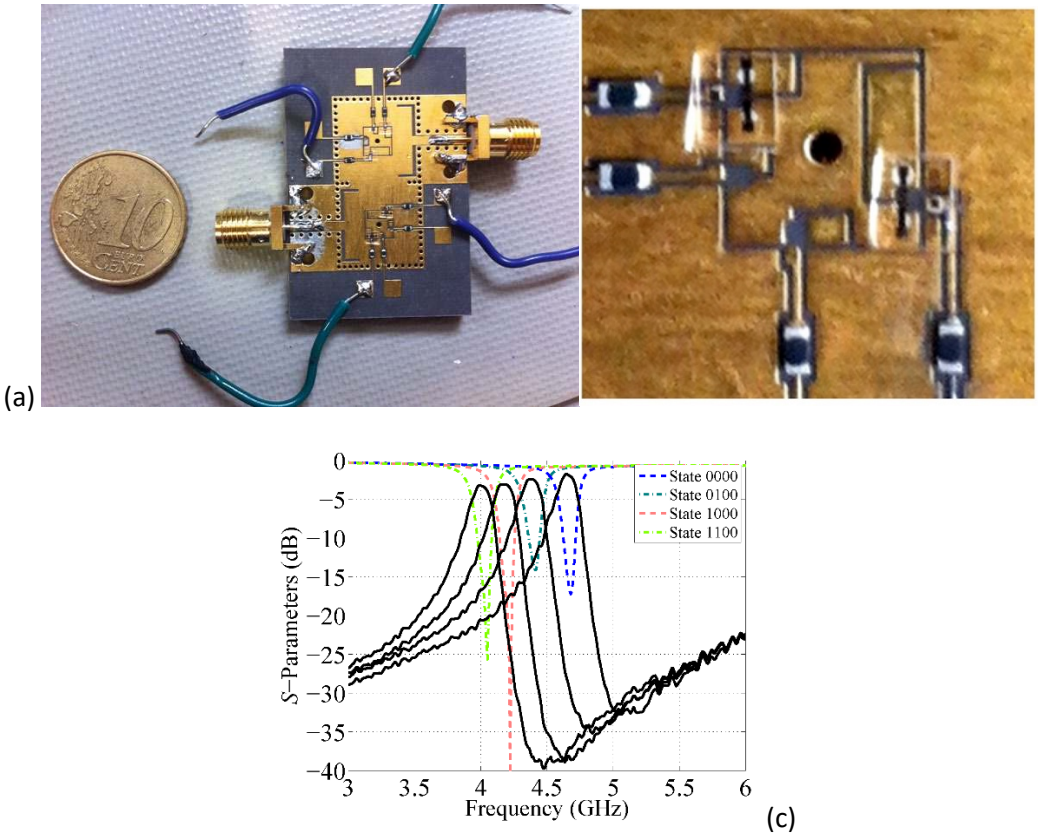

Figure 17: (a) Picture of the discretely tunable filter with four assembled RF MEMS resistive switches, (b) close-up image of the MEMS assembly on one resonator and (c) preliminary measurements for the four frequency states [67].

All of these characteristics are is clearly visible in the results of the digitally tunable 2-pole C-band bandpass filter implemented in 3.175 mm-thick Rogers 5880 that has been

proposed in [67], [69]. Four distinct bit capacitances are created in the capacitive patch, as shown in Fig. 17, providing up to 16 equally spaced narrow band frequency states within a single layer. To perform the frequency tuning, RF MEMS resistive switches from the XLIM research group of the University of Limoges (France) are mounted by means of a flip-chip assembly, thus avoiding the need for wire bonding. Such switches show a very good Q-factor (above 200 @ 1 GHz) and a reduced actuation voltage of 35 V.

Even though preliminary tests have been performed with only two RF MEMS switches assembled on each resonator, the achieved filter performance seems promising, particularly when taking into account the working frequency band. Specifically, such filters can be discretely tuned from 4 GHz in a 1100-state to 4.65 GHz in a 0000-state (i.e., tuning range = 15%) providing four equi-spaced responses with constant FBW around 2.5% and a measured Q_u of 105-205. Power handling capabilities have been also tested at 4.7 GHz, corresponding to the off-state MEMS position, which is the worst case in terms of self-actuation. The RF MEMS are able to handle up to 33.5 dBm before self-actuation occurs, which represents a remarkable advantange of this device with respect to other tuning solutions based on semiconductors.

Table 2 A comparison of the different types of tuning mechanisms applied to the coaxial SIW topology described in this review.

Type	Tuning Element	Frequency	Tuning Range	Q-factor	Complexity	Integrability
Analog [52-54], [56-59]	Varactor Diode	UHF L-band S-band	>30%	50-200	Low	High
Analog [65]	Trimmer Capacitor	UHF L-band S-band	>30%	100-200	Very low	High
Analog [63]	Linear actuator + Tuning disk	UHF L-band S-band	>50%	200-300	High	Poor
Digital [66]	PIN Diode	Up to C-band	<30%	100-150	Medium	Low
Digital [64-66]	RF MEMS	Up to X-band	<30%	100-200	Medium	High

Conclusions

Low-cost, high Q, and easy integration are well-recognized features of SIW technology. As reviewed and discussed in this paper, coaxial SIW technology enables the enhancement of some of these long-standing advantages, especially in terms of compactness, design flexibility, and easy tunability. Starting from a basic resonator, different fixed filters with simple and advanced responses have been discussed, as well as some of the more recent building blocks for implementing dual-mode filters as well as singlets and doublets. Finally, some examples of tunable coaxial SIW filters have been discussed in detail, and the main features of each approach are summarized in Table 2. In sum, very relevant size reductions can be achieved by capacitively loading a conventional SIW cavity resonator, obtaining good electrical performance, and

improving out-of-band rejection. Moreover, a broad range of coupling structures and topologies can be implemented, while keeping a very low cost and massive manufacturing process in single-layer PCB technology. Lastly, filter tunability can be easily performed due to the direct access to the capacitive part of the resonator, enabling the integration of different tuning elements such as trimmers, disks, varactors, PIN diodes, and RF MEMS.

Bibliography

[1] X.-P. Chen and K. Wu, “Substrate integrated waveguide filters: design techniques and structure innovations”, IEEE Microwave Magazine, vol. 15, no. 6, pp. 121 – 133, 2014.

[2] X.-P. Chen and K. Wu, “Substrate integrated waveguide filters: practical aspects and design considerations”, IEEE Microwave Magazine, vol. 15, no. 7, pp. 75 – 83, 2014.

[3] F. Grine, T. Djerafi, M.T. Benhabiles, K. Wu and M.L. Riabi, “High-Q substrate integrated waveguide resonator filter with dielectric loading”, IEEE Access, vol. 5, pp. 12526-12523, 2017.

[4] V. Sekar, M. Armendariz and K. Entesari, “A 1.2 – 1.6 GHz substrate-integrated-waveguide RF MEMS tunable filter”, IEEE Trans. Microwave Theory Tech., vol. 59, no. 4, pp. 866 – 876, 2011.

[5] S. Adhikari, Y.-J. Ban and K. Wu, “Magnetically tunable ferrite loaded substrate integrated waveguide cavity resonator”, IEEE Microw. Wireless Comon. Lett. , vol. 21, no. 3, pp. 139-141, 2011.

[6] S. Adhikari, A. Ghiotto and K. Wu, “Simultaneous electric and magnetic two-dimensional tuning of substrate integrated waveguide cavity resonator”, in IEEE MTT-S Int. Symp. Digest, 2012 pp. 1-3.

[7] N. Grigoropoulos, B.S. Izquierdo, R.P. Young, “Substrate integrated folded waveguides (SIFW) and filters”, IEEE Microw. Wireless Compon. Lett., vol. 15, pp. 829-831, 2005.

[8] L. Wu, L. Zhou, X.L. Zhou and W.Y. Yin, “Bandpass filter using substrate integrated waveguide cavity loaded with dielectric rod”, IEEE Microw. Wireless Compon. Lett., vol. 19, pp. 491-493, 2009.

[9] Y. Wang, W. Hong, Y. Dong, B. Liu, H.-J. Tang, J. Chen, X. Yin and K. Wu, “Half mode substrate integrated waveguide (HMSIW) bandpass filter”, IEEE Microw. Wiereless Compon. Lett., vol. 17, no. 4, pp. 265 – 267, 2007.

[10] Z. Zhang, N. Yang and K. Wu, “5-GHz bandpass filter demonstration using quarter-mode substrate integrated waveguide cavity for wireless systems”, in Proc. Of the 2009 IEEE Radio and Wireless Symposium, 2009, pp. 95 – 98.

[11] P. Li, H. Chu and R.-S. Chen, “Design of compact bandpass filters using quarter-mode and eight-mode SIW cavities”, IEEE Trans. Compon. Packagoing and Manufacturing Technology, vol. 7, no. 6, pp. 956 – 963, 2017.

[12] Q.-L. Zhang, W.-Y. Yin, S. He, L.-S. Wu, “Compact substrate integrated waveguide (SIW) bandpass filter with complementary split-ring resonators (CSRRs)”, IEEE Microw. Wireless Compon. Lett., vol. 20, no. 8, pp. 426-428, 2010.

[13] N. Delmonte, M. Bozzi, L. Perregrini and C. Tomassoni, “Miniaturization and Q-factor in substrate integrated waveguide cavities”, in Proc. 2018 IEEE MTT-S Int. Conf. on Numerical Electromagnetic and Multipysics Modeling and Optimization (NEMO), 2018, pp. 1 – 4.

[14] G.F. Craven and C.K. Mok, “The design of evanescent mode waveguide bandpass filters for a prescribed inserstion loss characteristic”, IEEE Trans. Microw. Theory Tech., vol. 19, no. 3, pp. 295-308, 1971.

[15] J.A. Ruiz-Cruz, Y. Zhang, K.A. Zaki, A.J. Piloto and J. Tallo, “Ultra-wideband LTCC ridge waveguide filters”, IEEE Microw. Wireless Compon. Lett., vol. 17, no. 2, pp. 115-117, 2007.

[16] L.-S. Wu, X.-L. Zhou and W.-Y. Yin, “Evanescent-mode bandpass filters using folded and ridge substrate integrated waveguides”, IEEE Microw. Wireless Compon. Lett., vol. 19, no. 3, pp. 161-163, 2009.

[17] H. Joshi, H.H. Sigmarsson, D. Peroulis, W.J. Chappell, “Highly loaded evanescent cavities for widely tunable high-Q filters”, in 2007 IEEE MTT-S Int. Microw. Symp. Dig., July 2007, pp. 2133–2136.

[18] H. Joshi, H. H. Sigmarsson, S. Moon, D. Peroulis, W.J. Chapell, “High-Q fully reconfigurable tunable bandpass filters”, IEEE Trans. Microw. Theory Tech., vol. 57, no. 12, pp. 3525-3533, 2009.

[19] V. Turgaliev, D. Kholodnyak, I. Vendik, D. Stöpel, S. Humbla, S. Müller, and M.A. Hein, “LTCC highly loaded cavities for the design of single- and dual-band low-loss miniature filters,” in Proc. of the 40th Europ. Microw. Conf., Sep. 2010, pp. 192-195.

[20] B. Schulte, V. Ziegler, B. Schoenlinner, U. Prechtel, H. Schumacher, “Miniaturized Ku-band filters in LTCC technology – evanescent mode vs. standard cavity filters”, in Proc. of the 40th Europ. Microw. Conf., Sep. 2010, pp. 5–8.

[21] J.C. Bohorquez, B. Potelon, C. Person, E. Rius, C. Quendo, G. Tanne and E. Fourn, "Reconfigurable planar SIW cavity resonator and filter", in 2006 IEEE MTT-S Int. Microw. Symp. Dig., June 2006, pp. 947–950.

[22] M. Armendariz, V. Sekar and K. Entesari, "Tunable SIW bandpass filter with PIN diodes", in Proc. of the 40th Europ. Microw. Conf., Sep. 2010, pp. 830-833.

[23] G.L. Matthaei, L. Young and E.M.T. Jones, Microwave Filters, Impedance-Matching Networks and Coupling Structures. New York: McGraw-Hill, 1964.

[24] J.D. Martínez, M. Taroncher, V.E. Boria, "Capacitively loaded resonator for compact substrate integrated waveguide filters", in Proc. of the 40th Europ. Microw. Conf., Sep. 2010, pp. 192-195.

[25] J.D. Martínez, S. Sirci, M. Taroncher, V.E. Boria, "Compact CPW-fed combline filter in substrate integrated waveguide technology", IEEE Microw. Wireless Compon. Lett., vol. 22, no. 1, pp. 7–9, 2012.

[26] J.B. Thomas, "Cross-coupling in coaxial cavity filters – A tutorial overview", IEEE Trans. Microw. Theory Tech., vol. 51, no. 4, pp. 1368-1376, 2003.

[27] S. Sirci, J.D. Martínez, J. Vague and V.E. Boria, "Substrate integrated waveguide diplexer based on circular triplet combline filters", IEEE Mcirow. Wireless Compon. Lett., vol. 25, no. 7, pp. 430-432, 2015.

[28] Z. Cai, K.-D. Xu, D. Lu, Y. Liu, and X. Tang, "A low phase noise oscillator using SIW combline resonator," in 2017 IEEE MTT-S Int. Microw. Symp. Dig., June 2017, pp. 1976–1978.

[29] D. Pozar, Microwave Engineering, 4th ed. Hoboken, NJ: John Wiley & Sons, 2012.

[30] H. J. Riblet, “An accurate approximation of the impedance of a circular cylinder concentric with an external square tube”, IEEE Trans. Microw. Theory Tech., vol. 31, no. 10, pp. 841-844, 1983.

[31] J. D. Martínez, S. Sirci, V. E. Boria, P. Martín-Iglesias, and H. Leblond, ``Practical considerations on the design and optimization of substrate integrated coaxial filters,'' in Proc. IEEE MTT-S Int. Conf. Numer. Electromagn. Multiphys. Modeling Optim. RF, Microw., THz. Appl. (NEMO), Seville, Spain, May 2017, pp. 299-301.

[32] A.P. Saghati, A.P. Saghati, and K. Entesari, “Ultra-miniature SIW cavity resonators and filters”, IEEE Trans. Microw. Theory Tech., vol. 63, no. 12, pp. 4329-4340.

[33] A. Anand, J. Small, M.S. Arif, M. Sinani, D. Peroulis and X. Liu, “A novel high-Qu octave-tunable resonator with lumped tuning elements”, in 2013 IEEE MTT-S Int. Microw. Symp. Dig., June 2013, pp. 1-3.

[34] F. Xu, K. Wu, “Guided-wave and leakage characteristics of substrate integrated waveguide”, IEEE Trans. Microwave Theory Tech., vol. 53, no. 1, pp. 66-73.

[35] X.-P. Chen, and K. Wu, “Substrate integrated waveguide cross-coupled filter with negative coupling structure,” IEEE Trans. Microwave Theory Tech., vol. 56, no. 1, pp. 142-149, 2008.

[36] B. Potelon, J. Favennec, C. Quendo, E. Rius, C. Person, and J. Bohorquez, “Design of a substrate integrated waveguide (SIW) filter using a novel topology of coupling,” IEEE Microw. Wireless Compon. Lett., vol. 18, no. 9, pp. 596-598, 2008.

[37] W. Shen, L.-S. Wu, X.-W. Sun, W.-Y. Yin, J.-F. Mao, “Novel substrate integrated waveguide filters with mixed cross coupling (MCC”, IEEE Microw. Wireless Compon. Lett., vol. 19, no. 11, pp. 701-703, 2009.

[38] K. Gong, W. Hong, Y. Zhang, P. Chen, and C.J. You, “Substrate integrated waveguide quasi-elliptic filters with controllable electric and mangnetic mixed coupling”, IEEE Trans. Microw. Theory Tech., vol. 60, no. 10, pp. 3071-3078, 2012.

[39] F. Zhu, W. Hong, J.X. Chen, and K. Wu, “Cross-coupled substrate integrated waveguide filtesr with planar resonators for system-on-package”, IEEE Trans. Compon. Packag. Manufact. Technol., vol. 3, no. 2, pp. 253-261, Feb. 2013.

[40] S. Sirci, M.A. Sánchez-Soriano, J.D. Martínez, V.E. Boria, F. Gentili, W. Bösch, and R. Sorrentino, “Design and Multiphysics analysis of direct and cross-coupled SIW combline filters using electric and magnetic coupling”, IEEE Trans. Microwave Theory Tech., vol. 63, no. 12, pp 4341-4353, 2015.

[41] S. Sirci, F. Gentili, J.D. Martínez, V.E. Boria, and R. Sorrentino, “Quasi-elliptic filter base don SIW combline resonators using a coplanar line cross-coupling”, in 2015 IEEE MTT-S Int. Microw. Symp. Dig., May 2015, pp. 1-4.

[42] D. Lu, T. Yan, X. Tang, “Compact quasi-elliptic combline filter in single-layered SIW technology with two tunable transmission zeros”, in Proc. of 17th Annual Wireless and Microw. Tech. Conf. (WAMICON), Apr. 2016, pp. 1-3.

[43] M.-H. Ho, J.-.C. Li, and Y.-C. Chen, “Miniaturized SIW cavity resonator and its application in filter design,” IEEE Microw. Wireless Compon. Lett., vol. 28, no. 8, pp. 651-653, 2018.

[44] S. Sirci, J.D. Martínez, V.E. Boria, “A novel magnetic coupling for miniaturized bandpass filters in embedded coaxial SIW,” Applied Sciences, vol. 9, no. 3, pp. 1-14, 2019.

[45] S. Saaedi, H. Sigmarsson, “Miniaturized evanescent-mode cavity SIW bandpass filter with spurious suppression”, in Proc. 2018 IEEE Radio and Wireless Symposium (RWS), Jan. 2018, pp. 234-236.

[46] R. M. Kurzrok, ‘’General three-resonator filters in waveguide," IEEE Trans. Microwave Theory Techn., vol. MTT-14, no. 1, pp. 46-47, 1966.

[47] M. Guglielmi, F. Montauti, L. Pellegrini, and P. Arcioni, “Implementing transmission zeros in the inductive-window bandpass filters,” IEEE Trans. Microw. Theory Tech., vol. 43, no. 8, pp. 1911–1915, Aug. 1995.

[48] X. P. Chen, K. Wu, and D. Drolet, ‘’Substrate integrated waveguide filter with improved stopband performance for satellite ground terminal," IEEE Trans. Microw. Theory Tech., vol. 57, no. 3, pp. 674-683, 2009.

[49] S. Bastioli, "Nonresonating Mode Waveguide Filters," in IEEE Microwave Magazine, vol. 12, no. 6, pp. 77-86, 2011.

[50] S. Amari, U. Rosenberg, and J. Bornemann, ``Singlets, cascaded singlets, and the nonresonating node model for advanced modular design of elliptic filters,'' IEEE Microw.Wireless Compon. Lett., vol. 14, no. 5, pp. 237-239, 2004.

[51] S. Sirci, M. A. Sánchez-Soriano, J. D. Martínez and V. E. Boria, "High Selectivity Filters in Coaxial SIW Based on Singlets and Doublets", in 2018 IEEE MTT-S Int. Microw. Symp. Dig., May 2018, pp. 704-707.

[52] S. Sirci, M.A. Sánchez-Soriano, J.D. Martínez, V.E. Boria, “Advanced filtering solutions in coaxial SIW technology base don singlets, cascaded singlets, and doublets”, IEEE Access, vol. 7, no. 1, pp. 29901-29915.

[53] M. A. Sánchez-Soriano, S. Sirci, J. D. Martínez, andV. E. Boria, ``Compact bandpass filters based on a new substrate integrated waveguide coaxial cavity,'' in Proc. IEEE MTT-S Int. Microw. Symp. Dig., San Francisco, CA, USA, May 2016, pp. 1-4.

[54] M. A. Sánchez-Soriano, S. Sirci, J. D. Martínez, andV. E. Boria, ``Compact dual-mode substrate integrated waveguide coaxial cavity for bandpass filter design,'' IEEE Microw. Wireless Compon. Lett., vol. 26, no. 6, pp. 386-388, Jun. 2016.

[55] S. Sirci, J. D. Martínez, M. Taroncher and V. E. Boria, "Varactor-loaded continuously tunable SIW resonator for reconfigurable filter design," in Proc. of 41st European Microwave Conference, Oct. 2011, pp. 436-439.

[56] S. Sirci, J. D. Martínez, M. Taroncher and V. E. Boria, "Analog tuning of compact varactor-loaded combline filters in substrate integrated waveguide," in Proc. of 42nd European Microwave Conference, Oct. 2012, pp. 257-260.

[57] A. Anand and X. Liu, “Substrate-integrated coaxial-cavity filter with tunable center frequency and reconfigurable bandwidth,” in Proc. IEEE 15th Annu. Wireless Microw. Technol. Conf. (WAMICON), Jun. 2014, pp. 1–4.

[58] I. C. Hunter and J. D. Rhodes, ‘’Electronically tunable microwave bandpass filters," IEEE Trans. Microw. Theory Techn., vol. 30, no. 9, pp. 1354-1360, Sep. 1982.

[59] S. Sirci, J. D. Martínez, R. Stefanini, P. Blondy, and V. E. Boria, ‘’Compact SMD packaged tunable filter based on substrate integrated coaxial resonators," in Proc. of IEEE MTT-S Int. Microw. Symp. Dig., Tampa Bay, USA, Jun. 2014, pp. 1-4

[60] A. Anand, Y. Liu and X. Liu, "Substrate-integrated octave-tunable combline bandstop filter with surface mount varactors," 2014 IEEE International Wireless Symposium (IWS 2014), X'ian, 2014, pp. 1-4.

[61] A. Anand and X. Liu, "Reconfigurable Planar Capacitive Coupling in Substrate-Integrated Coaxial-Cavity Filters," in IEEE Transactions on Microwave Theory and Techniques, vol. 64, no. 8, pp. 2548-2560, Aug. 2016.

[62] A. Anand, J. Small, D. Peroulis and X. Liu, "Theory and Design of Octave Tunable Filters With Lumped Tuning Elements," in IEEE Transactions on Microwave Theory and Techniques, vol. 61, no. 12, pp. 4353-4364, Dec. 2013.

[63] M. Abdelfattah and D. Peroulis, "A Novel Independently-Tunable Dual-Mode SIW Resonator with a Reconfigurable Bandpass Filter Application," in Proc. IEEE/MTT-S International Microwave Symposium (IMS), Philadelphia, PA, 2018, pp. 1091-1094.

[64] S. Sirci, M. A. Sánchez-Soriano, J. D. Martínez and V. E. Boria, "Electronically Reconfigurable Doublet in Dual-Mode Coaxial SIW," 2019 IEEE/MTT-S International Microwave Symposium - IMS, Boston, Massachusetts, 2019, pp. 1-4.

[65] D. Psychogiou and R. Gómez-García, "Multi-Mode-Cavity-Resonator-Based Bandpass Filters With Multiple Levels of Transfer-Function Adaptivity," in IEEE Access, vol. 7, pp. 24759-24765, 2019.

[66] S. Sirci, J.D. Martínez, and V.E. Boria, ”Low-loss 3-bit tunable SIW filter with PIN diodes and integrated bias network”, in Proc. 43st. Eur. Microw. Conf. (EuMW), Nuremberg, Germany, Oct. 2013, pp. 1211 − 1214.

[67] S. Sirci, E. Lemoine, A. Harck, J. D. Martínez, V. E. Boria, and P. Blondy, ‘’RF MEMS tunable SIW filter with 16-state digital responses," in Proc. of MEMSWAVE Inter. Workshop, La Rochelle, France, Jun. 2014, pp. 1-4

[68] S. Sirci, J. D. Martínez, V. E. Boria, P. Martín-Iglesias, ‘’Miniaturized substrate integrated coaxial filters with advanced and reconfigurable responses’’, in Proceeding of 2017 Microwave Technology and Techniques Workshop (MTT’17), ESA/ESTEC Noordwijk, The Netherlands.

[69] S. Sirci, J. D. Martínez, V. E. Boria, J. Gil and L. Marchand, "Design of Frequency Tunable LTCC Coaxial SIW Filters with Constant Passband Shape," 2018 IEEE MTT-S International Conference on Numerical Electromagnetic and Multiphysics Modeling and Optimization (NEMO), Reykjavik, 2018, pp. 1-4.